

# Craze-like damage in a core-shell rubber-modified epoxy system

HUNG-JUE SUE

Materials Science Group, Texas Polymer Center, B-1470, Dow Chemical USA, Freeport, TX 77541, USA

Toughening mechanisms of a core-shell rubber-modified epoxy were investigated using various microscopic techniques. It was found that the crack tip damage zone of the rubber-modified epoxy appeared to consist of multiple craze-like damage and massive shear banding using optical microscopy. The craze-like damage was further analysed using transmission electron microscopy (TEM) and actually found to be a collection of line arrays of highly cavitated rubber particles. The matrix material around the cavitated particles appeared to have plastically deformed, while the material outside of the array was undeformed. The structure and physical nature of this highly localized dilatational process are substantially different from those of the commonly known craze. The sequence of events leading to the formation of these craze-like line arrays is discussed.

## 1. Introduction

Toughening of ductile epoxies via elastomer modification has been known to be effective for more than two decades [1]. However, understanding as to how the ductile epoxies are toughened and what role(s) the elastomer plays in the toughening process have been actively debated since then [1-14].

In toughening epoxies, it is important to find out what toughening mechanisms are operative and under what circumstances they can be activated. Disputes over whether epoxy can undergo crazing or not are still not fully settled. Sultan and McGarry [1] suggested that crazing can be a predominant flow mechanism in rubber-modified epoxies when the rubber particle is large and the stress field is tensile. Lilley and Holloway [15] claim that crazing can occur in some fully cured epoxy resins. Yoshii and Bucknall [7-9] later show evidence of crazes in a carboxyl terminated butadiene and acrylonitrile (CTBN) rubber-modified epoxy matrix. They point out that the rate of crazing increases with the volume per cent of rubber particles, but is virtually independent of the degree of cross-linking of the resin. Morgan *et al.* [13] further propose that craze-crack growth does occur in crosslinked epoxies. On the other hand, Wronski and co-workers [16, 17], Narisawa *et al.* [14], Yee and Pearson [2, 3], Kinloch [5], and Sue [18] are not able to observe crazing in epoxy in their experiments. The work conducted by Yee and Pearson [2, 3] on CTBN rubber-modified epoxy systems clearly demonstrates that the major toughening mechanisms of rubber-modified ductile epoxy are cavitation of rubber particles, followed by shear banding of the matrix. Crazing is not observed. Occasionally, microcracks are found in the epoxy matrix [18, 19]. Without any convincing evidence showing the existence of crazes in fully cured

epoxies, it is generally believed that only when epoxy resins are either under-cured or have substantially low cross-link densities will crazing take place.

The objective of the present study focuses on revealing whether or not crazing can occur in a low cross-link density rubber-modified epoxy system. For this purpose, the DER<sup>®</sup> 332 epoxy resin cured with piperidine is used as the matrix material [2, 3, 5]. The core-shell rubber particles, which possess a uniform particle size and composition [20, 21], are utilized to toughen the epoxy matrix. The double notch-four point bend (DN-4PB) method [22] is employed to produce a sub-critically propagated crack. The sequence of failure events evolved from the sub-critically propagated crack of the DN-4PB specimen is investigated using various microscopic techniques. The causal relationship among the operative toughening mechanisms in this rubber-modified epoxy is also discussed.

## 2. Experimental procedure

The dynamic mechanical behaviour of both the neat resin and the core-shell rubber-modified epoxy was studied using dynamic mechanical spectroscopy (DMS) (Rheometrics<sup>®</sup> RMS-805) under a torsional mode, with 5 °C per step. A constant strain amplitude of 0.1% and a fixed frequency of 1 Hz were used. The samples were analysed at temperatures ranging from -150-200 °C. The temperature at which the tan  $\delta$  peak was located was recorded as the glass transition temperature,  $T_g$ .

The grafted-rubber-concentrate (GRC) core-shell rubber has a butadiene-styrene core with a multi-component shell [20, 21] and has a uniform particle size of approximately 100 nm. Ten weight per cent of

the rubber was added to the epoxy resin matrix. The rubber particles were mixed with the neat resin and degassed before the normal curing process was conducted. Five p.h.r. of piperidine was added to cure both the neat and rubber-modified epoxies at 120 °C for 16 h.

After the epoxy resin was cured and slowly cooled to room temperature (25 °C) in the oven, the 0.635 cm thick epoxy plaque was machined into bars with dimensions of 12.7 cm × 1.27 cm × 0.635 cm for the DN-4PB experiments (see Fig. 1 for the schematic of the DN-4PB geometry). These bars were then notched with a notching cutter (250 μm radius), followed by liquid nitrogen chilled razor blade tapping to wedge open a sharp crack. The ratio between the final crack length and the specimen width was held between 0.3 and 0.7 [23].

A Sintech-2 screw driven mechanical testing machine was used to conduct the DN-4PB experiments. A crosshead speed of 12.7 cm min<sup>-1</sup> was utilized. Care was taken to ensure that the upper contact loading points were touching the specimen simultaneously.

The damage zone of the survived DN-4PB crack was cut both along, and perpendicular to the thickness direction using a diamond saw (see Fig. 1). The plane strain core region was prepared for reflected light optical microscopy (ROM), transmitted light optical microscopy (TOM) and transmission electron microscopy (TEM) investigations. The fracture surface of the failed crack was coated with Au-Pd for scanning electron microscopy (SEM) investigation.

In the TOM investigation, thin sections (≈ 40 μm) of the GRC-modified epoxy were obtained by pol-

ishing, following the procedures described by Holik *et al.* [24]. The thin sections were taken from both the mid-section (plane strain region) and the surface (plane stress region) of the fractured DN-4PB specimens. These sections were made normal to the fracture surface but parallel to the cracking direction (Fig. 1). Further, in order to three-dimensionally observe the damage evolution, thin sections were also prepared perpendicular to both the fracture surface and the crack propagation direction. These thin sections were then examined using an Olympus Vanox-S optical microscope both under bright field and crossed-polarization.

In preparing the TEM samples, the core region of the damage zone was carefully trimmed to an appropriate size, i.e., an area of ≈ 5 mm × 5 mm, and embedded in DER 331 epoxy resin/diethylenetriamine (12:1 ratio by weight). The embedment was cured at 38 °C for 16 h. The block was further trimmed down to a size of about 0.5 mm × 0.5 mm with the damage zone roughly at the centre of the block. The block was then faced-off using a diamond knife and placed in a vial containing one gram of 99.9% pure osmium tetroxide (OsO<sub>4</sub>) crystals and stained for 72 h. It was found that the OsO<sub>4</sub> penetrated to a depth of about 1 μm. As a result, only the first few ultra-thin sections, which ranged in thickness from 60–80 nm, were well-stained and used for investigation. The thin sections were placed on 200 mesh, formvar-coated copper grids. The thin sections were examined using a Jeol 2000FX ATEM operated at an accelerating voltage of 100 kV.

### 3. Results

The present work focuses on studying the failure mechanisms of GRC-modified DER 332 epoxy resin/piperidine system. Also, the question of whether or not this rubber-modified epoxy system can undergo crazing is investigated.

The DMS results of both the neat and GRC-modified epoxies are shown in Figs 2 and 3. The dynamic mechanical behaviour of the two systems are effectively the same except for the enhanced low temperature relaxation peak and the drop of the storage modulus for the GRC-modified epoxy system at ≈ -80 °C. These effects are likely to be due to the low  $T_g$  (≈ -80 °C) nature of the butadiene-styrene

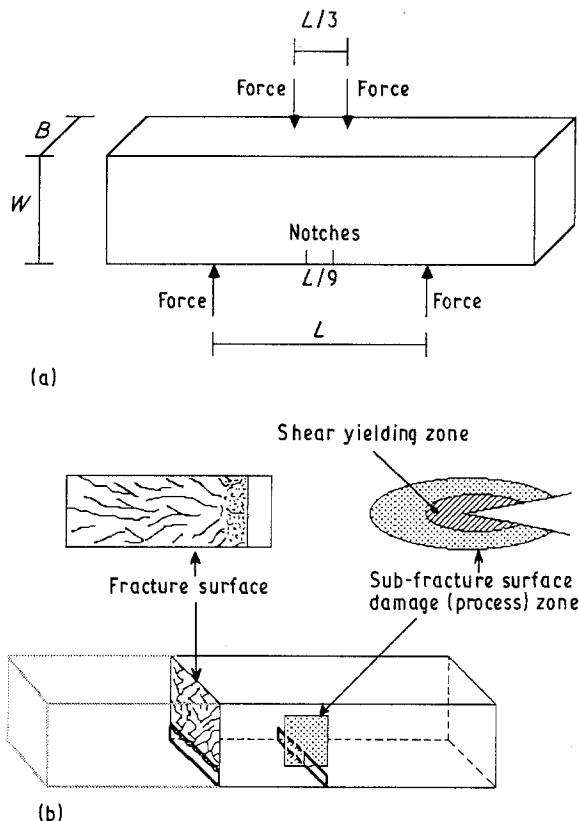


Figure 1 Schematics of: (a) the DN-4PB geometry and (b) the regions utilized for microscopy.

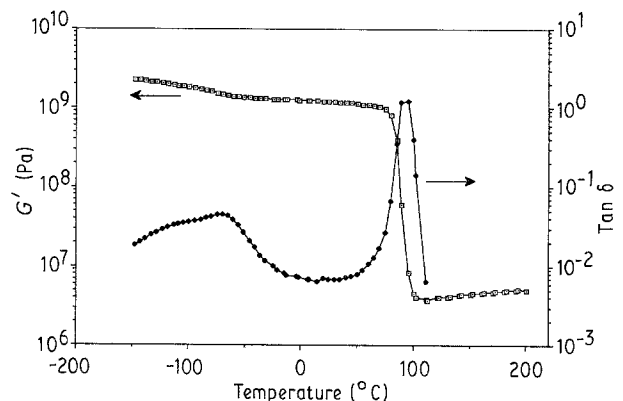


Figure 2 DMS of the DER 332 epoxy resin/piperidine system,  $T_g = 94$  °C.

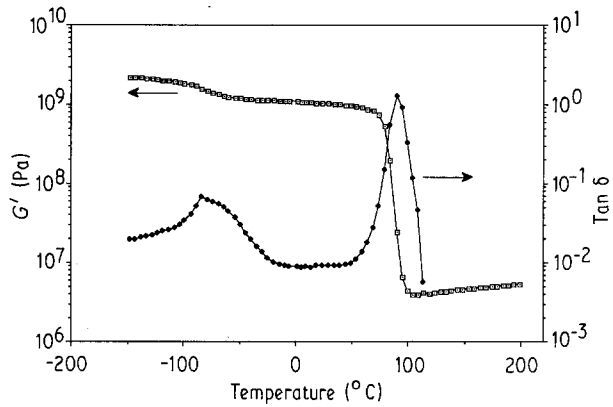


Figure 3 DMA of the DER 332 epoxy resin/piperidine/10% GRC system,  $T_g = 91^\circ\text{C}$ .

rubber in the core of the GRC particle. Since the  $T_g$  and the plateau modulus of the GRC-modified epoxy are nearly identical to those of the neat resin, the cross-link density of the matrix is probably not affected by the addition of the GRC particles. Therefore, the physical and mechanical properties of the matrix used in this study should be similar to those used by others in the literature [2, 3, 5, 6, 9, 19].

In order to study the failure mechanisms, the sub-critically propagated crack in the DN-4PB specimen, which is known to provide information concerning both the toughening mechanisms and sequence of failure events [22], is analysed using TOM. As shown in Fig. 4, a large damage zone is found in the plane strain region around the sub-critically propagated crack. This damage zone, which resembles the craze zones described by Chudnovsky [25] and Morelli and Takemori [26], appears to be composed of numerous crazes and/or microcracks. When the damage zone is viewed under crossed-polars, a smaller birefringent shear yielded zone surrounded by the large craze-like zone is also found (Fig. 4b). When ROM is used, the craze-like feature shown in Fig. 5 appears to further indicate the possible presence of crazes in the epoxy matrix. In the plane stress region (i.e. close to the surface region of the DN-4PB specimen), the craze-like damage, though smaller in size, appears to be still present (Fig. 6). To further investigate how the craze-like damage evolves in space, the thin section cut perpendicular to both the crack surface and the crack propagation direction in the damage zone is examined using TOM (Fig. 7). Analyses of both Figs 4 and 7 indicate that the craze-like damage is planar in nature. Toward the edge (i.e. the surface) of the specimen, the craze-like damage gradually diminishes in size and disappears at  $\approx 100\ \mu\text{m}$  away from the surface (Fig. 7b). Under the crossed-polars, birefringent shear bands are found around the surface (plane stress) region (Fig. 7c). This implies that the craze-like damage can take place only when the stress state is highly tri-axial. This also suggests that the photomicrograph shown in Fig. 6 is taken at a region which still possesses a rather high state of stress tri-axiality.

The craze-like damage feature shown above is highly unexpected in a fully cured epoxy system. To verify whether or not this cross-linked epoxy can

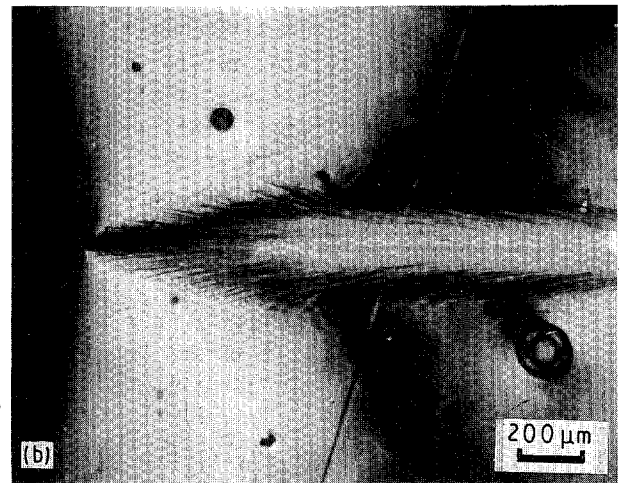
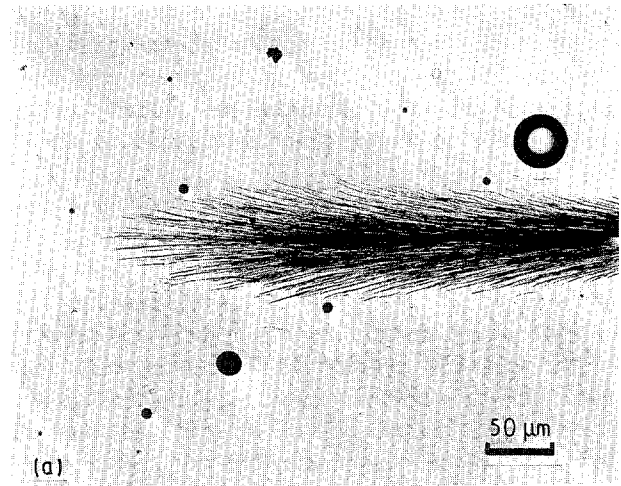


Figure 4 TOM of the plane strain damage zone of the GRC-modified epoxy taken: (a) under bright-field and (b) under crossed-polars. The crack propagates from right to left.

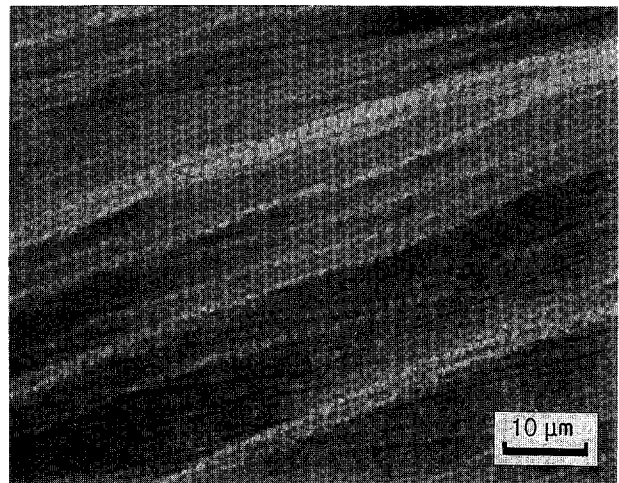


Figure 5 ROM of the craze-like pattern taken at the plane strain region. The crack propagates from right to left.

indeed undergo crazing, TEM investigations are conducted. At a low magnification, the TEM micrograph (Fig. 8) shows that the craze-like feature is similar to that shown in the ROM micrograph (Fig. 5). However, when a higher magnification micrograph is taken at various locations around the crack tip (Figs 9–12), the craze-like damage is found to be composed of

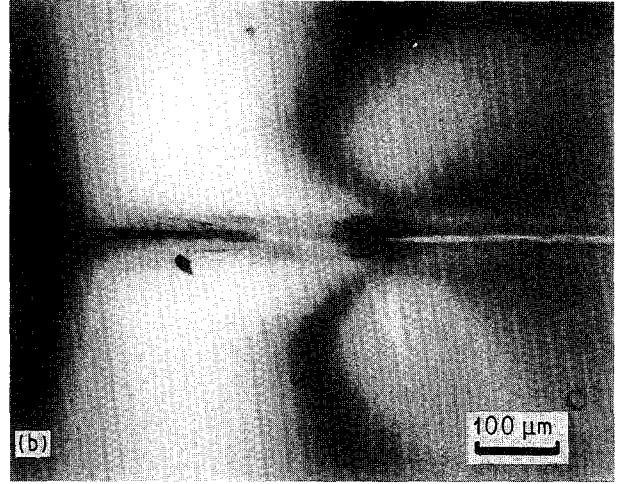
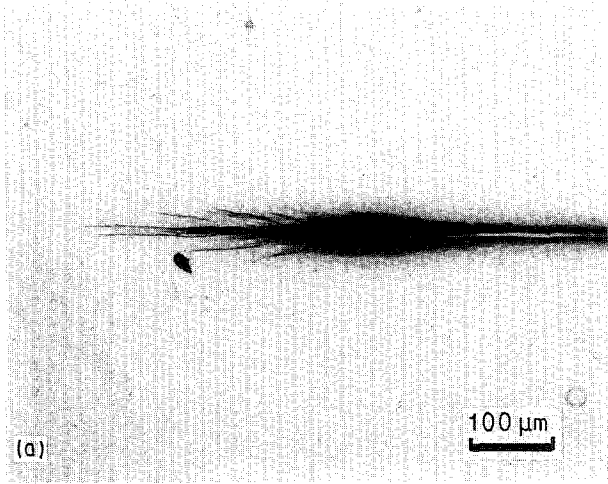


Figure 6 TOM at near the plane stress region of the GRC-modified epoxy taken: (a) under bright-field and (b) under cross-polars. The crack propagates from right to left.

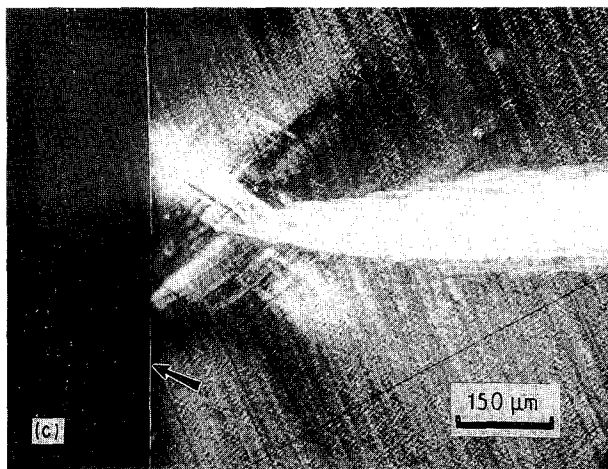
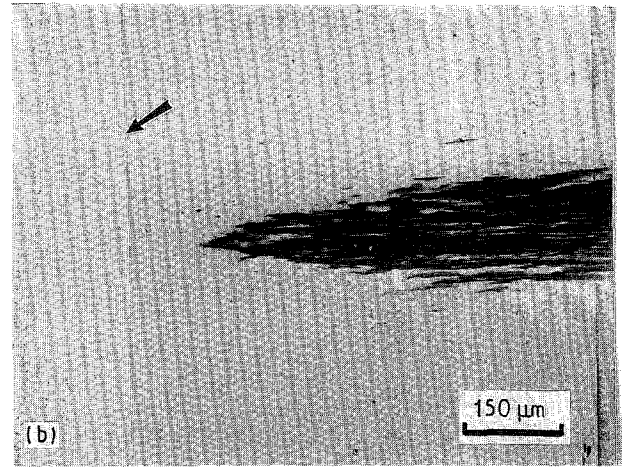
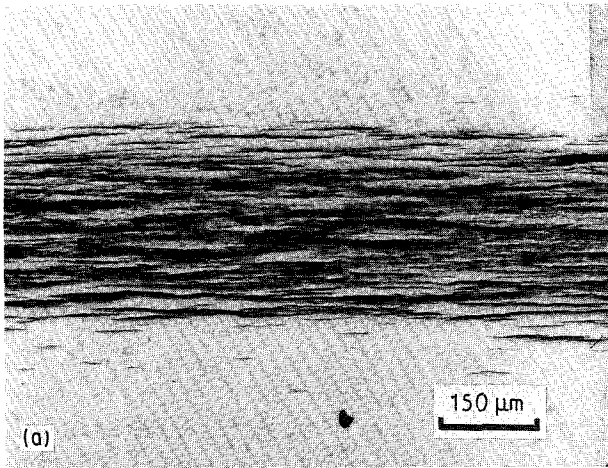


Figure 7 TOM micrographs taken from a thin section made normal to both the fracture surface and the crack propagation direction (i.e., the crack propagates toward the reader): (a) at the mid-section under bright-field (plane strain region); (b) at the edge under bright-field (plane stress region), and (c) same as (b) but viewed under crossed-polars. The arrow indicates the edge of the specimen surface.

numerous line arrays (they are planar in space, see Figs 4 and 7) of cavitated GRC particles. Since the particle cavitation line array is highly localized and extends approximately parallel to the crack propagation direction, it resembles the craze pattern at a low magnification. These cavitation line arrays are definitely not the same as the traditionally known crazes [8, 27–33]: no craze fibrils are found; no craze planes can be clearly defined; the material adjacent to

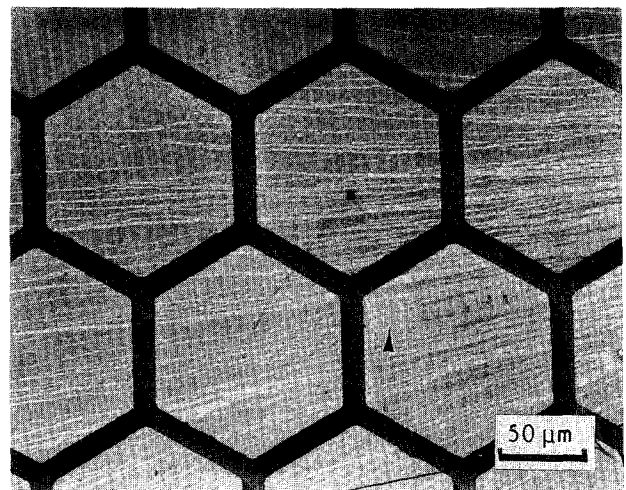


Figure 8 Low magnification TEM micrograph taken at the DN-4PB damage zone. The arrow indicates the crack tip. The crack propagates from right to left.

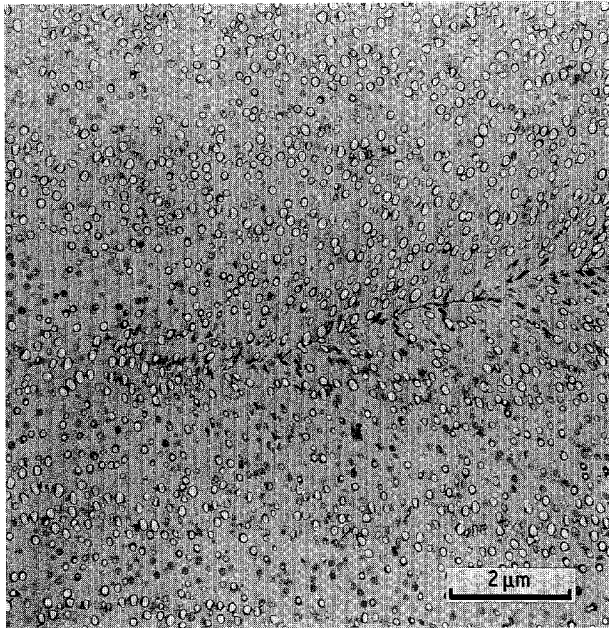


Figure 9 TEM micrograph taken at the crack tip of the DN-4PB damage zone. Large shear and dilatational plasticity are evident around the crack tip. The crack propagates from right to left.

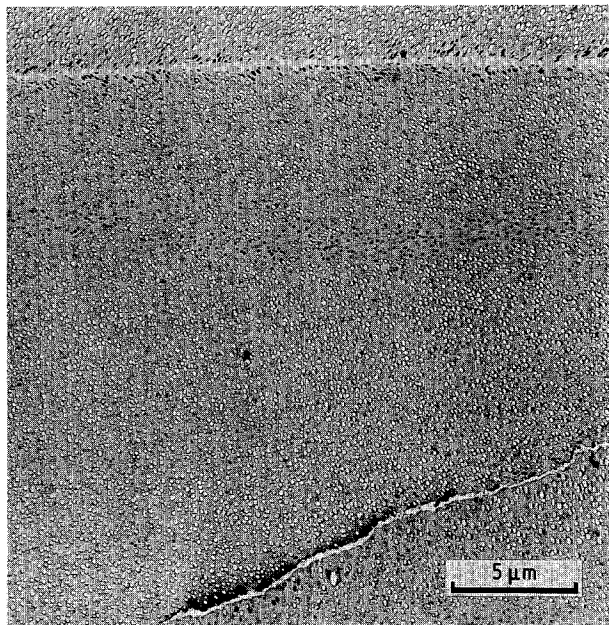


Figure 10 TEM micrograph taken at the crack wake of the DN-4PB damage zone. The crack shown on the right lower corner is a branched crack. The crack propagates from right to left.

the crack planes is highly shear yielded (Fig. 9). Coalescence of the cavitated particles into a microcrack is also observed (Fig. 13). The thickness of the line array can range in size from  $\approx 100$  nm, the size of a cavitated GRC particle (Fig. 12), to  $\approx 10$  μm (Figs 8–10) depending on the density of the line arrays. The finding of the large and distorted voids, in contrast to the intact GRC particles, indicates the occurrence of dilatational and shear plasticity of the neighbouring matrix inside the line arrays. For simplicity, these

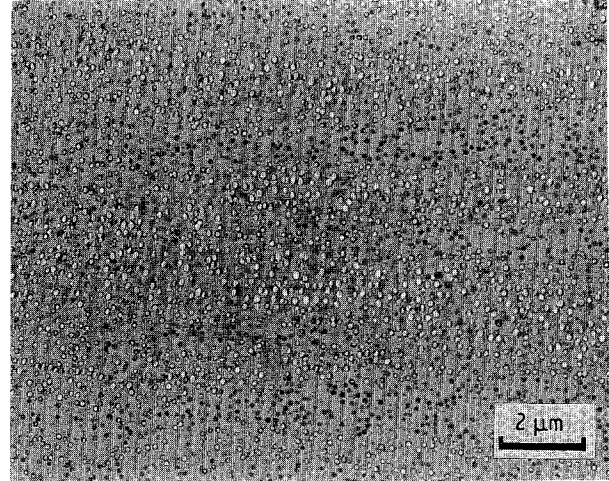


Figure 11 TEM micrograph taken beneath the crack plane of the DN-4PB damage zone. The crack propagates from right to left.

highly localized rubber particle-cavitation line arrays will hereafter be termed croids (derived from “crack” and “void”) in this work.

To further investigate how croids are formed, locations farther ahead of the crack tip, which will generally provide clues on how the crack tip damage evolves [18–21], are studied using TEM. The evolution of a croid, as shown in Fig. 14, appears to begin with the cavitation of statistically weak GRC particles. In a state of tri-axial stress the initial cavitation of the GRC particles could be caused by the high stress concentration due to local stress field overlap, i.e. particle–particle interaction, or simply by the presence of defect inside the GRC particles. Once they cavitate, the stress field due to the cavitated particle as well as the crack tip perturbation causes the croid to grow and propagate approximately parallel to the crack propagation direction (or perpendicular to the major principal stress direction), as shown in Figs 15 and 16. These observations suggest that the croid mechanically initiates and grows in a manner similar to that of a craze. For clarity, a schematic summarizing the mechanism of croid formation is shown in Fig. 17. Further, locations of the TEM micrographs taken in Figs 9–16 are indicated in Fig. 18.

#### 4. Discussion

Since the first observation of crazes in glassy polymers [26], studies on kinetics [28, 29], microstructure [30], mechanisms [31–33], mechanics and physics [34–40] of crazes have been extensively conducted. Unfortunately, these studies are not fully applicable to the understanding of the croiding behaviour. Although the physical differences between the craze and croid behaviours are apparent, the mechanisms on how the craze and croid form are quite similar, as pointed out in the previous section. As a result, some physics and mechanics that are used to describe craze formation are also considered in an attempt to explain croid formation.

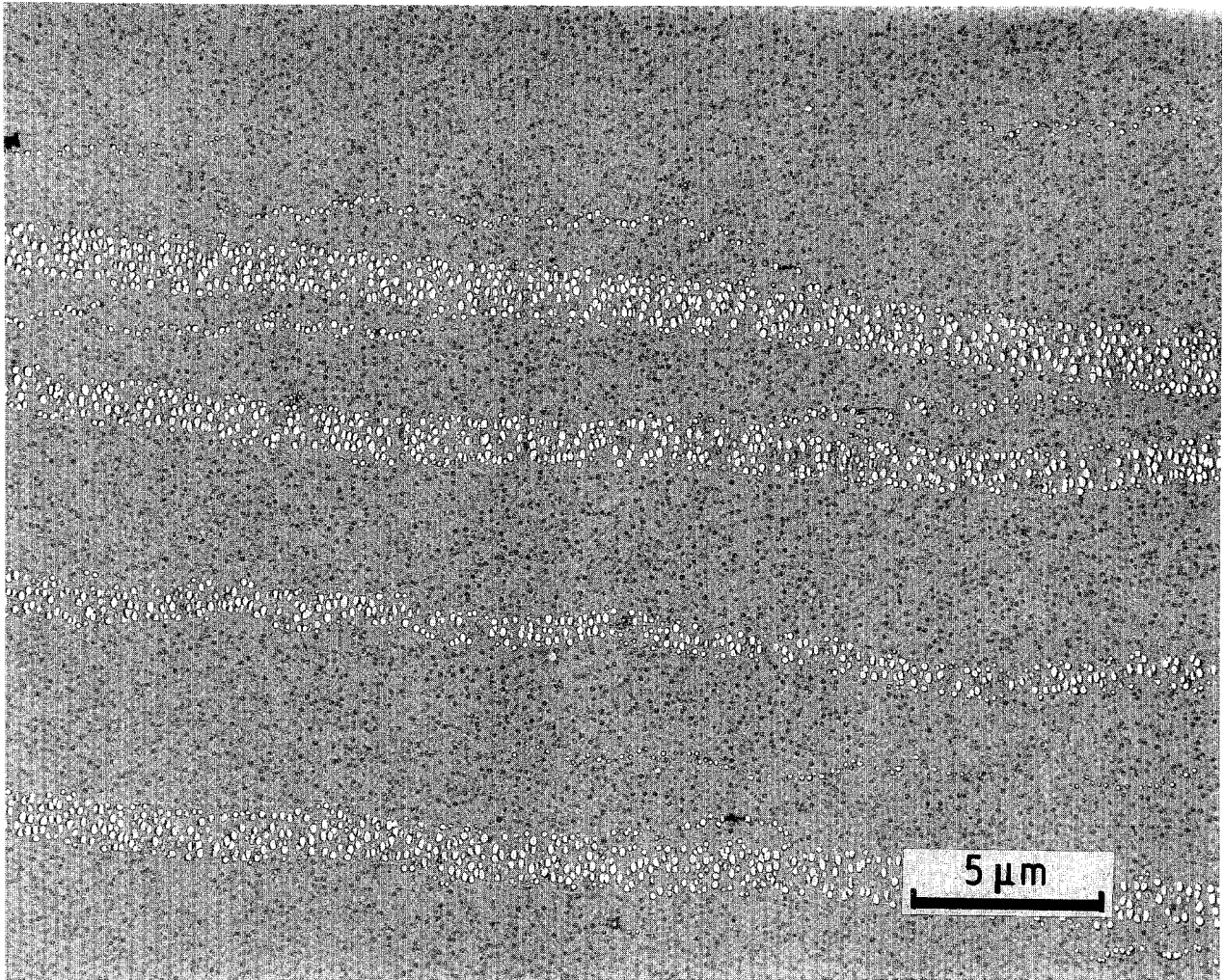


Figure 12 TEM micrograph taken further beneath the location shown in Fig. 11 of the DN-4PB damage zone. The crack propagates from right to left.

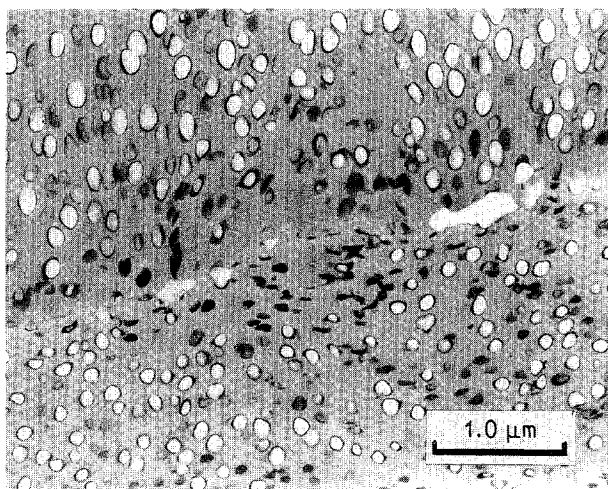


Figure 13 TEM micrograph taken beneath the crack wake of the DN-4PB damage zone. A microcrack is observed and appears to evolve from the coalescence of voids inside the croid. The crack propagates from right to left.

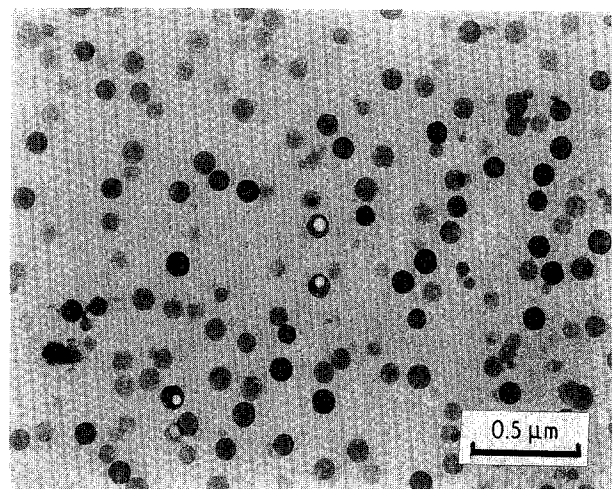


Figure 14 TEM micrograph taken far away from the crack tip of the DN-4PB damage zone. Only scattered cavitated GRC particles are observed. The crack propagates from right to left.

Observation of the croids in a low cross-link density, but fully cured, rubber-modified epoxy is highly unexpected. The studies conducted by Yee and Pearson [2, 3, 19] and Kinloch [5] on a similar epoxy matrix, while toughened by different rubber tougheners, do not produce the same type of failure mech-

anisms. Even with the same epoxy matrix and curing conditions, when the epoxy is modified with dispersed acrylic rubber [41, 42] (instead of the GRC particle), the major failure mechanism is dominated by extensive shear banding rather than croiding [43]. Consequently, the formation of the croid, rather

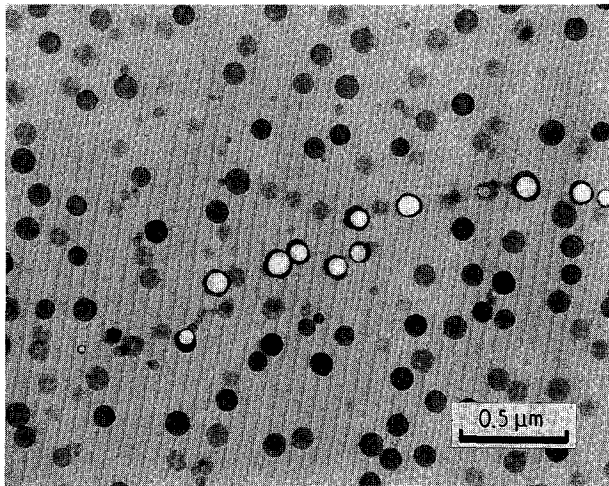


Figure 15 TEM micrograph taken closer to the crack tip (than that of Fig. 14) of the DN-4PB damage zone. The voids begin to link as a croid. The crack propagates from right to left.

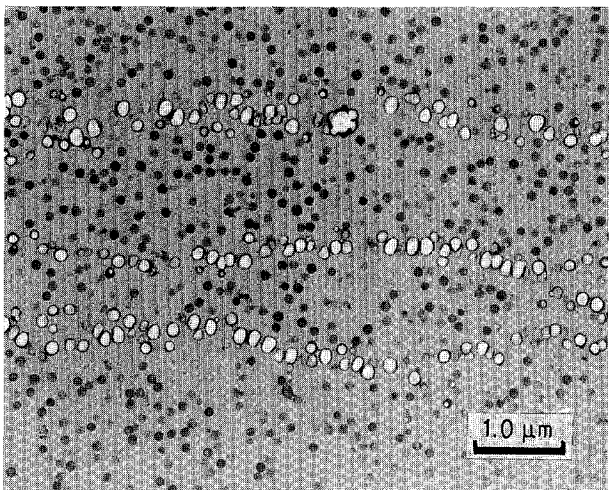


Figure 16 TEM micrograph taken closer to the crack tip (than that of Fig. 15) of the DN-4PB damage zone. Mature croids are formed. The crack propagates from right to left.

than the expected circular cavitation zone or micro-cracking/multiple cracking [2, 3, 18, 19], must be strongly affected by the toughener phase and/or the intrinsic property of the matrix. The present paper only focuses on revealing how the croid is formed. Characterization of the physical and mechanical properties of both the toughener phase and the matrix, which will probably help explain why croiding occurs in this system while it is not observed in others [2, 3, 19], will be conducted and reported in the future.

Theories used to describe how crazes initiate and grow [38–40, 44] are examined in an attempt to explain the possible cause(s) of croid formation. Gent [39], Haward [40], and Andrews and Bevan [38] propose different views on how a craze is formed. Gent proposes that the formation of voids is caused by the formation of a thin yielded zone ahead of the crack tip. The stress state within this zone is highly tri-axial due to the elastic constraint of the surrounding material. Consequently, the voids form [39]. Haward [40] and Andrews and Bevan [38] regard the hydrostatic stress

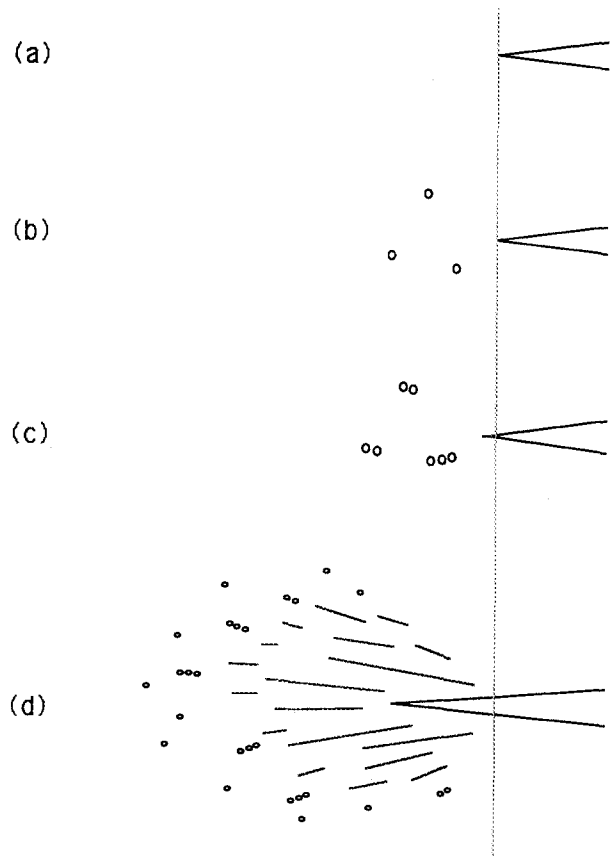


Figure 17 Sketched sequence of events of croid formation: (a) the initial starter crack; (b) cavitation of the weak GRC particles in front of the crack tip when the specimen is initially loaded; (c) once the voids form in front of the crack tip, the GRC particles around the equatorial region of the void begin to cavitate; as a result, the croid forms and (d) when the crack grows, steps (a)–(c) repeat themselves and the croids grow approximately parallel to the crack propagation direction. Note that the size is not drawn to scale.

for void growth as the controlling parameter. They, however, agree that crazing is caused by voiding and controlled by the hydrostatic tension in the polymer [45]. Argon further suggests that three sequential stages are distinct for craze formation: thermally activated production of stable microporosity under stress, formation of a craze nucleus by plastic expansion of holes in a small region while elastically unloading the surroundings, and extension of the craze nucleus into a planar yield zone [44]. The croiding in the GRC-modified D.E.R. 332 epoxy resin/piperidine system cannot be satisfactorily interpreted by the above theories. The croid is initiated from the cavitation of the statistically weak GRC particles far away from the crack tip (Fig. 14). Cavitation of the weak GRC particles must be caused by the hydrostatic tension which, in turn, is induced by the mode-I crack tip stress field [46]. No discernable thin yielded zone is found around these cavitated GRC particles. Upon cavitation of the weak GRC particles, the stress concentration and contour immediately adjacent to the cavitated GRC particles are altered substantially [47, 48]. If the matrix intrinsically possesses a low resistance to dilatational plasticity (or cracking) but is unable to undergo crazing, then the most likely route to relieve the dilatational stress is by means of cavitation of the neighbouring GRC particles around the equatorial

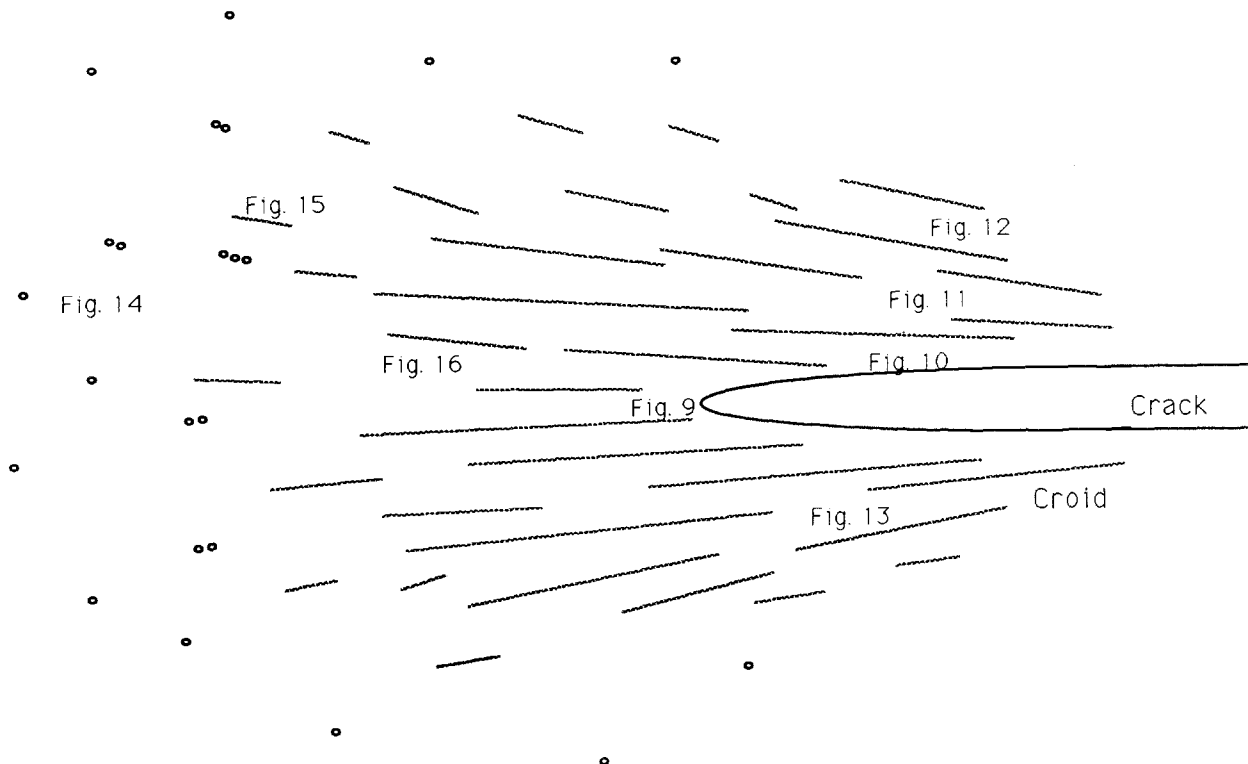


Figure 18 Schematic showing the locations where Figs 9–16 were taken in the damage zone.

region with respect to the major principal stress direction [47–49]. As a result, instead of causing the possible microcracking and premature failure of the matrix, croids form (Fig. 15).

Croids resemble crazes in their orientation with respect to the major principal stress direction [20, 38–40, 44], i.e. croids grow perpendicular to it. The reason is probably due to a series of events. Mechanically, the maximum principle stress at the equatorial region of a GRC particle increases abruptly when the particle is cavitated in front of the crack tip [47, 48]. The intact GRC particles near the cavitated particles then preferentially cavitate, because the cavitation strength of the GRC particle is probably lower than that of the matrix. The interaction of neighbouring voids (see Fig. 17c) due to stress field overlap effectively acts like a crack, which is called a croid in this study. Consequently, the growth of the croid is governed by the major principal stress [49] as in the case of craze and crack growth.

Croids appear to grow both along and opposite the crack propagation direction, depending on the location of the croids with respect to the main crack and the nature of the surrounding morphology (Figs 12 and 15). Once a croid forms, the surrounding material is relieved from further dilatation. Hence, the neighbouring GRC particles appear to be intact. When croids grow close to each other, they merge as thick croids. The matrix material inside the thick croids is relieved of any geometric constraint. Consequently, plastic shear deformation, which is evidenced by the large distortion of the cavitated GRC particles (Figs 9–12) as well as the birefringence pattern observed under crossed-polars (Fig. 4), also takes place after the formation of the dense croids. This phenomenon is analogous to the notion made by Yee and Pearson

[2, 3], namely, that the tri-axial stress has to be relieved for the formation of shear bands around the highly constrained sharp crack tip. Therefore, the major toughening mechanisms in the GRC-modified DER 332 epoxy resin/piperidine system are likely to be croiding, followed by shear yielding of the matrix. It is noted that, owing to the complexity of the local stress field around the cavitated GRC particles, it is difficult to estimate under what circumstance the geometric constraint can be relieved. The elastic constraint, which induces further stress tri-axiality, may also play an important role in the formation of shear bands. Finite element methods that take the material non-linearity into account have to be employed to help predict the conditions for croid and shear band formation.

When the dominant stress state is either uni-axial [43] or bi-axial, croiding appears to be inoperative (Fig. 7). In other words, a critical state of stress tri-axiality may have to be reached for croids to initiate. This indicates that croiding is different from crazing (crazing does occur on the bulk specimen surface and thin films [7]) in terms of the requirement for the state of stress tri-axiality for initiation. The study may also imply that the yield stress of the matrix is greatly raised above the brittle stress of the matrix (or the brittle stress of the matrix is reduced enormously) under the state of stress tri-axiality. As a result, the only route to avoid catastrophic failure is through croiding of the system. The above speculation still awaits support from further experimental effort.

The microcracks observed in this GRC-modified epoxy appear to be initiated by the coalescence of voids inside the croid (Fig. 13). These microcracks either grow and terminate as short cracks or join the main crack and disappear (Figs 9, 13 and 19). The

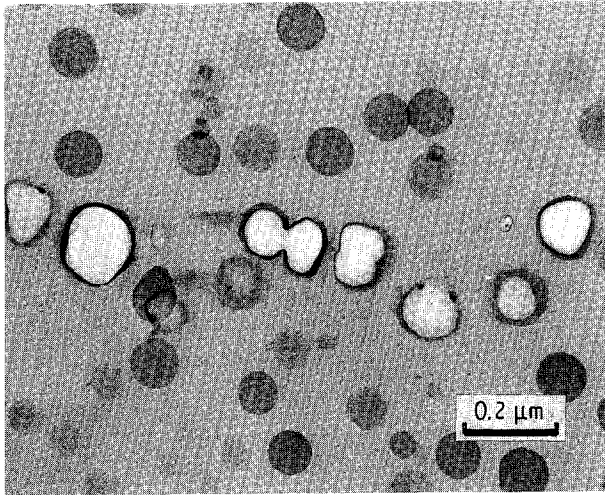


Figure 19 TEM micrograph taken inside the DN-4PB damage zone. The volume of the cavity can reach as much as 250% of the volume of an intact GRC particle.

evolution of these microcracks from the croid seems to be analogous to that of the craze-crack mechanism [8, 13, 30, 38–40]: the croid is thickened by the growth of voids (Figs 12, 15 and 16); accordingly, the ligaments between the voids also are stretched thinner and eventually broken apart (Figs 13 and 19). As a result, the microcrack forms.

In order to verify the reproducibility of the croid formation, many batches of sample plaques are cast and examined at various testing rates [43]. It is found that croids form in all conditions tested (however, the size of craze-like damage, which relates to the fracture toughness, depends strongly on the testing rates [43]). The main reason why the croid was not observed in the past by other investigators could have been due to the inadequate use of tools. Traditionally, investigation of failure mechanisms has been focused on fracture surface studies using SEM. When the stress-whitened zone on the fracture surface of rubber-modified ductile epoxies is studied using SEM, only voids produced from the cavitated rubber particles are observed [1, 4–7]. When the fracture surface of the GRC-modified DER 332 epoxy is studied using SEM, indeed, only voids are found (Fig. 20). No evidence of croid formation can be observed. Consequently, it is conceivable that the croids may have existed in some

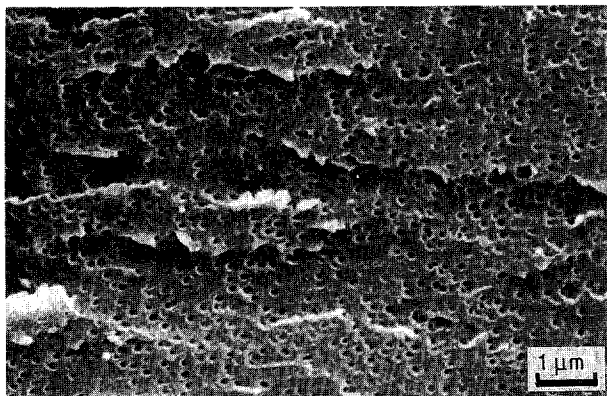


Figure 20 SEM micrograph taken on the stress-whitened zone of the GRC-modified epoxy.

of the rubber-modified systems studied by others. Further research has to be conducted to check whether or not croiding can also occur in other thermo-setting polymers.

It is noted that the majority of the GRC particles in the damage zone are either fully cavitated or undeformed. This kind of highly localized large particle internal cavitation process is very different from those reported in the literature [2, 3, 5, 19, 47], where cavities are largest near the crack plane and gradually diminish in size away from the crack. The size of the cavity inside the croid is also substantially bigger than that observed inside the circular cavitation zone [18, 19, 47]. This implies that the matrix has plastically dilated to a higher degree around the cavitated particles. The amount of plastic dilatation in the matrix can reach as high as 250% (i.e., volume of the cavity divided by volume of the intact GRC particle), as shown in Fig. 19. Such plastic dilatation of the matrix exists throughout the damage zone. As a result, the contribution of the plastic dilatation in the toughening of this GRC-modified epoxy is probably as significant as, if not more than, the shear plasticity.

It is also noted that the GRC particles at the crack wake appear to be darker than those away from the crack plane. This phenomenon has also been observed in many rubber-modified systems we studied previously [18, 21]. A possible cause of such an artifact is the over-staining of the rubber particles around the crack wake, which provides an easy route for the  $\text{OsO}_4$  to penetrate into the system. Hence, darker GRC particles are found along the crack planes.

## 5. Conclusion

The failure mechanisms of the GRC-modified DER 332 epoxy resin/piperidine system were studied. It was found that the damage zone around the crack tip consisted of numerous croids (line arrays of cavitated rubber particles). The formation of massive croids relieves the local constraint and, as a result, promotes shear yielding of the matrix. These croids are physically different from the traditionally known crazes. The mechanisms on how croids are formed are nevertheless similar to those of the crazes. The event that initiates the formation of croids is found to be cavitation of statistically weak GRC particles away from the crack tip. Owing to the abrupt increase of the maximum principal stress at the equatorial region of the cavitated particles as well as the low resistance of the matrix to dilatational plasticity, the cavities grow approximately along the crack propagation direction. Consequently, the croids form.

## Acknowledgement

The author would like to thank Professors A. F. Yee and R. A. Pearson for their valuable discussions on this work. Special thanks are given to E. I. Garcia-Meitin, N. A. Orchard, W. L. Huang, D. M. Pickelman, C. C. Garrison, R. E. Jones, D. L. Barron, K. Sehanobish, and C. Bosnyak for their support, discussion, and for supplying the materials.

## References

1. J. SULTAN and F. McGARRY, *Polym. Eng. Sci.* **13** (1973) 19.
2. A. F. YEE and R. A. PEARSON, *J. Mater. Sci.* **21** (1986) 2462.
3. *Idem*, *ibid.* **21** (1986) 2475.
4. A. C. GARG and Y. W. MAI, *Comp. Sci. Technol.* **31** (1988) 179.
5. A. J. KINLOCH, in "Advances in Polymer Science", edited by K. Dusek, Vol. 72 (Springer-Verlag, Berlin, 1986) p. 45.
6. W. BASCOM, R. TING, R. J. MOULTON, C. K. RIEW and A. R. SIEBERT, *J. Mater. Sci.* **16** (1981) 2657.
7. C. B. BUCKNALL and T. YOSHII, *British Polym. J.* **10** (1978) 53.
8. C. B. BUCKNALL, in "Toughened Plastics" (Applied Science, London, 1977) p. 221.
9. T. YOSHII, PhD Thesis, Cranfield, UK, 1975.
10. F. J. GUILD and R. J. YOUNG, *J. Mater. Sci.* **24** (1989) 2454.
11. S. KUNZ-DOUGLASS, P. W. R. BEAUMONT and M. F. ASHBY, *ibid.* **16** (1981) 2657.
12. S. BANDYOPADHYAY, *Mater. Sci. Eng.* **A125** (1990) 157.
13. R. J. MORGAN, E. T. MONES and W. J. STEELE, *Polymer* **23** (1982) 295.
14. I. NARISAWA, T. MURAYAMA and H. OGAWA, *ibid.* **23** (1982) 291.
15. J. LILLEY and D. G. HOLLOWAY, *Phil. Mag.* **28** (1973) 215.
16. A. S. WRONSKI and M. PICH, *J. Mater. Sci.* **12** (1977) 28.
17. A. S. WRONSKI and T. V. PARRY, *ibid.* **17** (1982) 2047.
18. H.-J. SUE, *Polym. Eng. Sci.*, **31** (1991) 275.
19. R. A. PEARSON, PhD Thesis, Ann Arbor, Michigan, 1990.
20. D. E. HENTON, D. M. PICKELMAN, C. B. ARENDS and V. E. MEYER, US Patent 4 778 851, 1988.
21. H.-J. SUE, E. I. GARCIA-MEITIN, D. M. PICKELMAN and P. C. YANG, in "ACS Book Series", edited by C. K. Riew, 1991.
22. H.-J. SUE, R. A. PEARSON, D. S. PARKER, J. HUANG and A. F. YEE, *Polymer Prepr.* **29** (1988) 147.
23. O. L. TOWERS, in "Stress Intensity Factors, Compliances, and Elastic  $\eta$  Factors for Six Geometries" (The Welding Institute, Cambridge, UK) 1981, p. 1.
24. A. S. HOLIK, R. P. KAMBOUR, S. Y. HOBBS and D. G. FINK, *Microstruct. Sci.* **7** (1979) 357.
25. A. CHUDNOVSKY, NASA Report CR-174634, 1984.
26. T. A. MORELLI and M. T. TAKEMORI, *J. Mater. Sci.* **18** (1983) 2047.
27. J. A. SAUER, J. MARIN and C. C. HSIAO, *J. Appl. Phys.* **20** (1949) 507.
28. E. E. ZIEGLER and W. E. BROWN, *Plast. Technol.* **1** (1955) 341.
29. Y. SATO, *Kobunshi Kagaku*, **23** (1966) 69.
30. R. P. KAMBOUR and A. S. HOLIK, *J. Polym. Sci.* **7** (1969) 1393.
31. J. MURRAY and D. HULL, *Polymer* **10** (1969) 451.
32. A. S. ARGON and SALAMA, *Phil. Mag.* **35** (1977) 1217.
33. R. P. KAMBOUR, *J. Polym. Sci.: Macromol. Rev.* **7** (1973) 1.
34. S. S. STERNSTEIN and L. ONGCHIN, *Polym. Prepr.* **10** (1969) 1117.
35. R. J. OXBOROUGH and P. B. BOWDEN, *Phil. Mag.* **28** (1973) 547.
36. A. P. WILCZYNSKI, C. H. LIU and C. C. HSIAO, *J. Appl. Phys.* **48** (1977) 1149.
37. A. S. ARGON and J. G. HANNOOSH, *Phil. Mag.* **36** (1977) 1195.
38. E. H. ANDREWS and L. BEVAN, *Polymer* **13** (1972) 337.
39. A. N. GENT, *J. Mater. Sci.* **5** (1970) 925.
40. R. N. HAWARD, in Proceedings of the International Symposium of the Physics of Non-crystalline Solids, Sheffield, 1970, Preprint.
41. D. K. HOFFMAN and C. B. ARENDS, US Patent 4 708 996, 1987.
42. *Idem*, US Patent 4 789 712, 1988.
43. H.-J. SUE, E. I. GARCIA-MEITIN and N. A. ORCHARD, in preparation.
44. A. S. ARGON, *Pure Appl. Chem.* **43** (1975) 247.
45. E. H. ANDREWS, in "The Physics of Glassy Polymers", edited by R. Haward (Applied Science Publishers, London, 1973) p. 442.
46. J. G. WILLIAMS, in "Fracture Mechanics of Polymers" (Ellis Horwood Ltd., New York, 1984) p. 124.
47. H.-J. SUE, PhD Thesis, The University of Michigan, Ann Arbor, 1988.
48. C. L. HOM and R. M. McMEEKING, *J. Mech. Phys. Solids* **37** (1989) 395.
49. I. M. WARD, in "Mechanical Properties of Solid Polymers", 2nd Edn (Wiley & Son, New York, 1983) p. 419.

Received 12 February  
and accepted 20 June 1991